How to Cite:
Reddy, G. P., & Ramashri, T. (2022). MRI brain tumor early detection, classification and performance evaluation using KFCM and SVM. *International Journal of Health Sciences*, *6*(S6), 6663–6675. https://doi.org/10.53730/ijhs.v6nS6.11219

MRI brain tumor early detection, classification and performance evaluation using KFCM and SVM

Gangadhara Reddy P.
Research Scholar, Department of ECE, Sri Venkateswara University College of Engineering, S.V. University, Tirupati, A.P., India
*Corresponding author Email: gangadharareddy.p@gmail.com

Ramashri T.
Professor, Department of ECE, Sri Venkateswara University College of Engineering, S.V.University, Tirupati, A.P., India

Abstract---A tumor-infected brain is a dreadful illness. It is an area in the brain caused by cell development irregularity. An infected brain area might be challenging to identify and categorize using the MR imaging approach. Images of human brain anatomy are resulted using various imaging methods. Strange brain compositions are difficult to detect using standard image processing methods. MRI differentiates and explains the human neurological design. This research proposed an analytical method for detecting brain tumors. As a result, the brain tumor early diagnosis technique is crucial for reducing mortality rates. We propose a computer-aided radiology system that will analyze brain tumors from MRI data to diagnosis. We constructed a model that uses FCM and Kernel FCM to segment the MRI images and DWT to extract features and the SVM network to classify tumors.

Keywords---MRI, segmentation, FCM, KFCM, DWT, SVM.

Introduction

In human body, brain is a primary processing organ that governs cognition, memory, vision, and respiration. Millions of cells stack in a rigid cranium to protect the brain from external forces. The brain stem is the genesis of this vital organ. Thus, any anomaly in the brain may endanger human health. Brain tumors are the most serious of these disorders. The treatment of brain tumors varies depending on their location, size, and kind. The most frequent therapy for brain tumors is surgery, which has no neurological adverse effects [1]. Several methods, including computed tomography (CT) scanning, magnetic resonance imaging (MRI), and electroencephalography (EEG), are used to diagnose brain

International Journal of Health Sciences ISSN 2550-6978 E-ISSN 2550-696X © 2022.
Manuscript submitted: 9 April 2022, Manuscript revised: 27 June 2022, Accepted for publication: 18 July 2022

tissues. MRI technology employs a magnetic field and radio waves to display pictures of inside organs. Due to the excellent resolution of this approach, the images offer vital information on brain tissue structure [2]. Since manual categorization of MRI images is difficult and error-prone in complex circumstances, MRI imaging identifying brain tumors and comparing their tissues to healthy cells is not a simple process, should be performed by a trained professional [3].

The critical issue was detecting a brain tumor in the early stages to adopt proper treatment. Based on these data, the best radiation, surgery, or chemotherapy may be chosen. Consequently, early detection of a tumor increases the odds of a patient's survival. Using imaging modalities, the segmentation identified the afflicted tumor portion [4]. An image is segmented into pieces with similar colour, texture, contrast, and border properties. Feature extraction is a quantitative evaluation of medical images that assess a structure or tissue's pathology. Feature extraction is a specific case of dimensionality reduction. They are utilized for handwritten digit identification, speaker identification, text categorization, and medical applications [5-6].

An automated MRI medical image loading system is critical to producing quick and accurate findings. This approach uses novel Computer Aided Diagnosis (CAD) to assist clinicians and radiologists in identifying and categorizing brain tumors. Experts in radiology diagnostic and medical imaging increasingly use CAD to classify brain tumors [7]. Overall, this approach consists of three stages: reducing image noise, segmenting the tumor area, and extracting characteristics from the segmented image. Finally, labelled MRI images are used to train a classifier to predict tissue changes [8]. The general flow diagram of brain tumors classification presents in figure1. This figure shows the stages involved in pre-processing and segmenting medical MRI images, extracting features, selection of features, and using machine learning algorithms [9-10]. The following subsections describe each stage in detail.

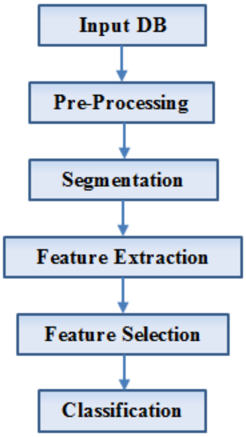

Figure 1. Overall flow diagram of brain tumor detection and classification

Data Acquisition

The first step in image formation is an image acquisition of raw imaging data. This data is converted and stored in digital format. Imaging methods include X-rays, positron emission tomography (PET), magnetic resonance imaging (MRI), computed tomography (CT), and ultrasound. The X-ray emits high radiation levels that might cause cancer and skin problems. But PET works by detecting radiation from a radiotracer and injecting it into the human's organ suitably. On the other hand, MRI uses powerful magnets to create a magnetic field that can display an organ from all perspectives [11]. This device has two modes of operation: high field for high-quality images and low field for quick diagnosis. This technique accurately detects brain tumors, strokes, and hemorrhages.

Pre-processing

Tumor detection begins with image pre-processing, which requires a significant amount of time and effort from researchers. This phase aims to improve image quality and remove noise and labels like time and date [12]. This approach involves cropping, resizing, histogram equalization, filtering, and normalization.

Segmentation

A cluster or segmentation approach builds a collection of entities so that entities in the same cluster are more similar than entities in other clusters. Clusters are continuous parts of multi-dimensional space with high density compared to other similar areas with moderate density. Clustering is the arrangement of pixels in an image that affects attributes such as brightness [13]. Hard clustering simply fits one data item into one cluster. Soft clustering allows data objects to belong to several clusters.

Feature Extraction

Extraction of an image feature determines the most essential properties in MR images. Condensing an image data collection is known as "feature extraction". Adding a step like an image classification will speed up the processing time. A well-chosen group of characteristics may be sufficient for a broad categorization of a lesion. Images and objects are analyzed to find the most notable features that are typical of a wide variety of item kinds. Classifiers use these attributes to classify them. Feature extraction seeks to identify qualities that distinguish across different input plans. When a feature extraction is conducted, it must output the image characteristics into a collection of feature vectors [14-15]. The Shape Intensity Index (SII) retrieves shape and intensity proofs utilizing Correlation, Contrast, Homogeneity, Entropy, Mean, Variance, Standard deviation, Skewness and Kurtosis.

Classification SVM

It's an excellent supervised learning approach for data analysis and categorization, and it learns rapidly even from large volumes of data. It may be utilized for two or more categorization difficulties [7, 8]. This approach is based on the division plane theory to divide data into subgroups depending on class membership. It helps to detect and classify MR brain tumors. The system includes training and assessment [16-17]. The SVM can train and assess feature vectors for unstructured and semi-structured data. The SVM classifier exhibits class overlap. Additionally, it is vulnerable to noisy feature vectors. Although parametric classification methods take longer to run owing to their mathematical complexity, they are more accurate and consistent when working with small samples. Our suggested versions SVM-RBF and SVM-Linear use the structural risk reduction approach were compared to existing algorithms [18]. The paper's main contribution is:There are two new frameworks for MRI brain tumor image classification: SVM-RBF and SVM-Linear.

- Mask construction, cross-validation, ranking, change classification, underfitting, and overfitting are handled by the SVM-RBF and SVM-Linear, respectively.
- Data classification using SVM-linear and non-linear SVM-RBF may minimize computation load.
- SVM-RBF and SVM-Linear have higher accuracy and reliability than previous approaches.

Methodology proposed

Image Preprocessing

In MRI, preprocessing improves signal-to-noise ratio (SNR), contrast enhancement, noise reduction, smoothing, and sharpening. The brain image is median filtered to increase the input image quality [19]. Figure 2 shows the approach used to classify a brain MR images. Here preprocessing, segmentation, feature extraction, feature reduction, training, database storage, and testing are used.

Morphological Techniques for Image Segmentation

This article uses morphological techniques (MT) to segment data to reorganize pixels according to their relative worth. Erosion and dilation are the most accessible operation here. This is done by comparing each pixel's value to all other pixels nearby, much like dilation.

Fuzzy-C-Means (FCM) Clustering

In the FCM technique, only local information is used for segmentation. The membership functions of data items are strongly associated with respective clusters and cluster centres (group focuses). Each cycle improves the group's focus and membership function [20]. The FCM's primary goal is to minimized by equation 1.

$$F(x,y) = \sum_{i=1}^{m} \sum_{j=1}^{n} (\mu_{i,j}{}^{f}) \left\| U_i - V_j \right\|^2 \qquad (1)$$

Where:

m – The amount of information
v_j – Group focuses
f – Fuzziness index f ϵ [1, ∞]
n – Total number of group focuses
μ_{ij} – Information emphasises to group focuses membership function
d_{ij} – The Euclidean distance between ith information focuses and jth group focuses
$\left\|U_i - V_j\right\|^2$ – is the Euclidean distance between the ith information focuses and jth information focuses.

Kernelised FCM Clustering (KFCM)

The KFCM technique addresses the limitation of FCM to handle minor changes across clusters. Input data are transformed nonlinearly into a high-dimensional feature space [21]. Kernel-based approaches deal with arbitrary non-linear mappings from R^d to higher-dimensional spaces (kernel space). Kernel space has potentially limitless dimensions. An optimal linear classifier in kernel space may not be optimal in feature space. This is why the dimensions are increased. Finally, the kernel technique exploits K's dot product expression in kernel space [21]. KFCM clustering implements fuzzy C-means clustering in a high-dimensional feature space after non-linearly translating the input model space R^s. The most common nonlinear transformation is a Mercer kernel function. The two most common kinds are polynomials and radials. Assume that $X = \{x_1, x_2, \ldots\ldots, x_n\} \subset R^q$ is a feature data space. R^s is mapped to a feature space sample data set R^q, where c is the number of classes to split, 2≤c≤N, and the following objective function is used:

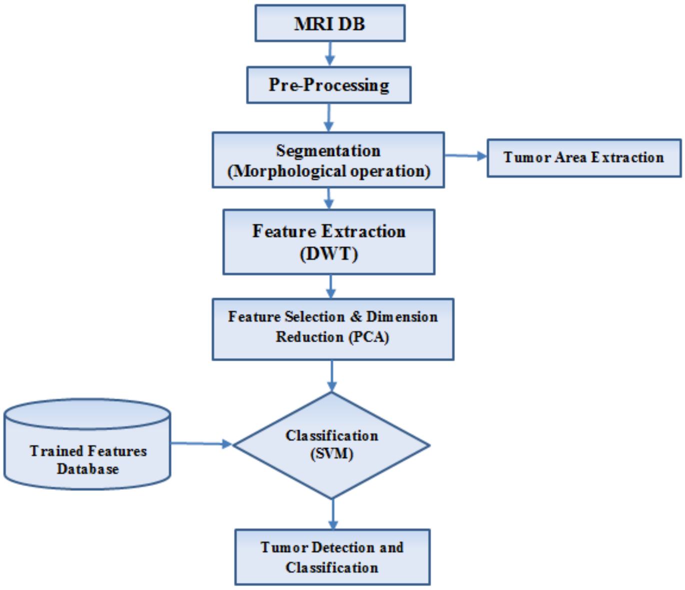

Figure 2. Overall architecture for proposed methodology

$$J_{km}(U,V) = \sum_{i=1}^{c} \sum_{j=1}^{N} \mu_{ij}^{m} \left\|\psi(x_j) - \psi(v_i)\right\|^2 = \sum_{i=1}^{c} \sum_{j=1}^{N} \mu_{ij}^{m}\, d_{kij}^{2}(x_j - v_i) \qquad (2)$$

K=1,2,3….Nand i=1,2,3….c

Where, m is the fuzzy control index. If the kernel function K is used, the Euclid distance between the feature space R^q and the vectors xi and x_j may be expressed as follows:

$$d_{Kij} = \left[K(x_i, x_i) - 2K(x_i, x_j) + K(x_j, x_j)\right]^{½} \qquad (3)$$

Iteration of Equations (15)-(16) provides the smallest value of the resulting objective function generated by the Lagrange multiplier optimization algorithm:

$$\mu_{ij} = \frac{\left({}^{1}\!/_{d_{kij}^{2}(x_j, v_i)}\right)^{{}^{1}\!/_{m-1}}}{\sum_{i=1}^{c}\left({}^{1}\!/_{d_{kij}^{2}(x_j, v_i)}\right)^{{}^{1}\!/_{m-1}}} \qquad (4)$$

$$v_i = \frac{\left({}^{1}\!/_{d_{kij}^{2}(x_j, v_i)}\right)^{{}^{1}\!/_{m-1}}}{\sum_{i=1}^{N}\left(\mu_{ij}^{m} K(x_j, v_i)\right)} \qquad (5)$$

The loop is completed when $\|U^{k-1} - U^{k}\| \le \boldsymbol{\varepsilon}$, the final partition matrix U, and the cluster centre matrix V are discovered. The KFCM technique may cluster various data structures, but it provides no structural information about the class.

Feature Extraction

DWT based Extraction of Features

The wavelet is a robust mathematical tool used to extract the wavelet coefficients of MR images. The Wavelet transform is an image decomposition approach that allows various channels to represent picture features with unique frequency sub-bands at many scales. Pictures may be transformed from the spatial to the frequency domain [22]. Figure 3 depicts two-level decomposition. The four parts of the picture that may be separated vertically and horizontally are labelled LL, LH, HL, and HH.

Where:

Lo_D – low pass filter;
Ho_D-high pass filter;
$2\downarrow 1$ - Downsampling columns;
$1\downarrow 2$ – Downsampling rows;

The wavelet coefficient from MRI brain images is extracted using DWT. The DWT algorithmic logic can convert spatial frequency to time-based field frequency.

$$Xc_{i,j}(z) = DS\left[\sum_{z} A(z) k_i^{*}(z - 2^{ij})\right] \qquad (6)$$

$$Yc_{i,j}(z) = DS\left[\sum_{z} A(z) l_i^{*}(z - 2^{ij})\right] \qquad (7)$$

$Xc_{i,j}$ and $Yc_{i,j}$ show the specific details of the coefficients and their constituents. A high-pass filter (l(n)) is the opposite of a low-pass filter (k(n)). In this scenario, 'j' and 'i' represent the two independent variables, wavelet calibration and translation. The signal A(n) is given to the coefficient of estimate Xc(n) and the detail component Yc (n).

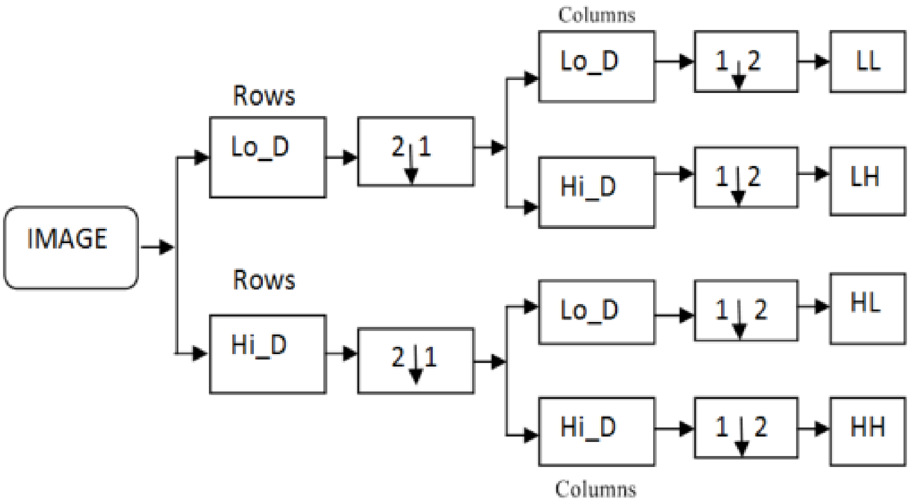

Figure 3. 2D Discrete wavelet transform

Principal Component Analysis (PCA)

PCA is a method for reducing the number of dimensions necessary for obtaining the most significant variance. It all begins with the guy who has a large amount of data. The set is examined to check whether there are any unconnected linkages between the points. It begins with the Eigenvectors of the covariance matrix of the input data, which are utilised to generate the vectors [23]. In multivariate data analysis, the extra dimensions, or PCs, may be used to explore the dataset in a new way. Look for PCs with the highest Eigenvalues and then choose them to get a smaller dimension

SVM Based Tumor Classification

A novel machine learning system based on statistical learning theory has recently been suggested called Support Vector Machine (SVM). Hyperplanes are created in multidimensional space to organize training data. Fitting kernels for hyperplanes, RBF, polynomials, and linear classifiers [23-24] may be employed. Hyperplanes try to segregate positive and negative examples to reduce the distance between classes. SVMs are the most often used learning systems. It has been utilized successfully in scientific applications like RNA sequencing to solve clustering issues instead of neural networks. The data are divided into two groups by an N-dimensional hyperplane. Data occurrences in training and testing are usually small. Each instance has one "target value" (class labels) and many "attributes" (features).

$(X,Y)=\{(x_1,y_1),(x_2,y_2),(x_3,y_3),\ldots\ldots,(x_n,y_n)\}$shows a training set where $x_n \in R_y^N \; and \; y_n \in \{-1,+1\}$. SVM requires the solution of the following optimization problem [17]:

$$\min_{w,b,\xi} \frac{1}{2} w^T w + C \sum_{i=1}^{l} \xi_i \qquad (8)$$

Subject to $y_i(w^T \emptyset(x_i) + b) \geq 1 - \xi_i \;\;, \;\; \xi_i \geq 0$

The function translates xi into a higher (possibly infinite) dimensional space. Then SVM identifies the best linear separating hyperplane in this higher-dimensional space. The term C > 0 error penalty parameter $K(x_n,y_n) = \phi(x_i)- \phi(x_j)$ is also called the kernel function. The kernel converts data from the input to the feature space. The four primary kinds of kernel functions are:

$Linear: K(x_i, x_j) \ = x_i^T$ (9)
$Polynomial: K\left(x_i, x_j\right) = \ (\gamma x_i^T x_j + r)^d$ (10)
$Radial\ Basis\ Function(RBF): K\left(x_i, x_j\right) = \quad \exp\left(-\gamma \left\|x_i - x_j\right\|^2,\ \gamma > 0\right.$ (11)
$Sigmoid: K(x_i, x_j) \ = \tanh\left(\gamma x_i^T\ x_j + r\right)$ (12)
Here, γ, r and d are kernel properties.
We propose to make use of a kernel known as Gaussian RBF, which is defined by
$K\left(x_i, x_j\right) = \exp\left(-\frac{\left\|x_i - x_j\right\|^2}{2\sigma^2}\right.$ (13)

In SVM,**σ =** is the kernel's width. SVM's over-fitting and under-fitting may be eliminated by varying the width **σ** of the training set. Global kernels, such as polynomial kernels, are insufficient for image classification since the association between image pixels is confined. Roy, Bet.al employed the Gaussian RBF kernel in this study, inspired by the promising findings of the RBF kernel in brain tumor [25].

Results and Discussion

The suggested segmentation and classification methods for a brain tumor were developed using the Matlab programme. First of all, the KAGGLE dataset is a real-world clinical dataset, which contains 22 brain MR DICOM slices. Zenodo datasets from 10 individuals with roughly 200 brain parts were also used in this study. Four MR brain images are acquired for the purpose of segmentation. For experimentation, 256 x 256 MR images are used as the standard. KFCM and FCM segmentation findings for four MRI brain images are given in Figure 4, including an original MR image, the calculated tumor area, and a segmented image of the brain. Image 4e in figure 4 reveals the needed segmented image. Figure 4 shows the results of MR image segmentation.

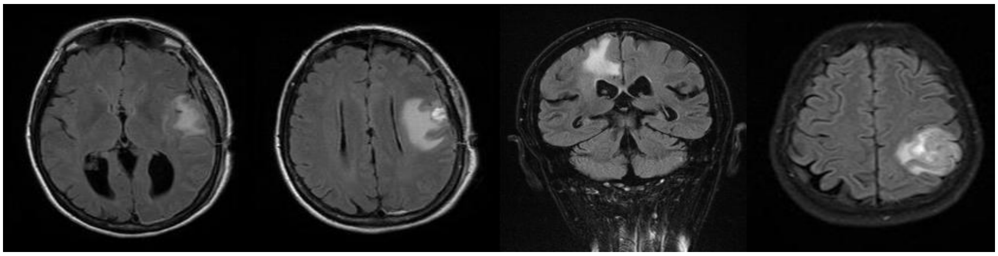

4a. Input Images

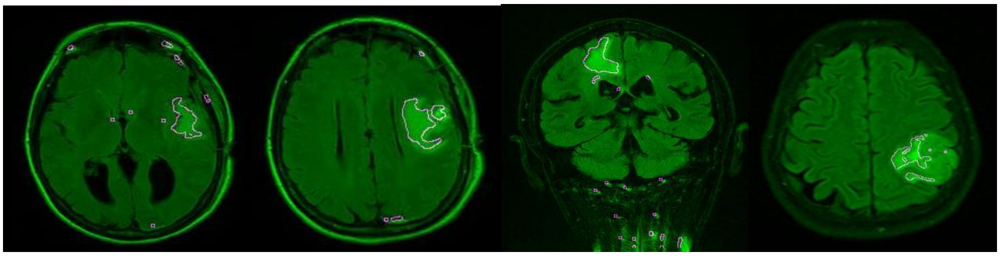

4b. Tumor area detection after FCM Segmented

4c. FCM Segmented Images

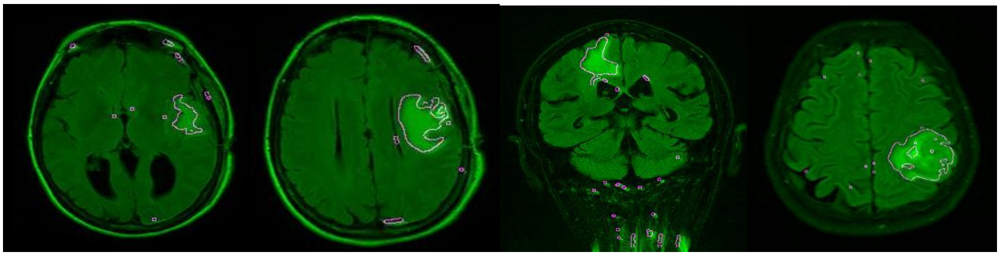

4e. Tumor area detection after KFCM Segmented

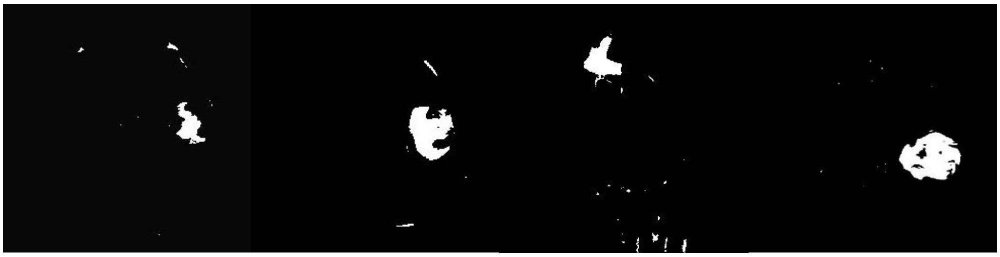

4e. KFCM Segmented Images

Figure 4. The input images, tumor detection and Segmented images obtained from FCM and Kernel FCM

The performance characteristics of the suggested technique, such as tumor area, number of pixels, and accuracy in various SVM classifiers, are calculated. Table 1 displays the collected performance metrics. For the MR image, Daubechies 3 level decomposition is used to identify wavelet coefficients, which are subsequently reduced in dimension using the PCA technique. Using these coefficients, a Gray level co-occurrence matrix is then created

Table 1
Simulated Performance Analysis

Algorithms	Fuzzy C-means_ SVM				Kernel FCM _SVM			
Images	i1_Brain1	i2_Brain2	i3_Brain3	i4_Brain4	i1_Brain1	i2_Brain2	i3_Brain3	i4_Brain4
Tumor Area	0.008287	0.012474	0.012191	0.007068	0.149328	0.001195	0.015933	0.02447
Number of Pixel	659	992	1010	1437	11875	95	320	4975
Accuracy of Linear kernel	55.0000	65.0000	60.0000	70.0000	50.0000	60.0000	40.0000	55.0000
Accuracy of RBF kernel	70.0000	70.0000	80.0000	80.0000	50.0000	70.0000	40.0000	60.0000
Accuracy of Polynomial kernel	50.0000	60.0000	63.3300	60.0000	50.0000	66.6600	36.6600	50.0000

Table 2
Feature extraction from MR images of the brain

Algorithms	Fuzzy C-means _SVM				Kernel FCM _SVM			
Images	i1_Brain1	i2_Brain2	i3_Brain3	i4_Brain4	i1_Brain1	i2_Brain2	i3_Brain3	i4_Brain4
Contrast	0.288462	0.315197	0.27907	0.250333	0.235929	0.321764	0.188134	0.183902
Correlation	0.153456	0.152753	0.177357	0.146174	0.136052	0.172128	0.144728	0.114707
Energy	0.870594	0.892825	0.86371	0.926688	0.833962	0.913118	0.802934	0.903261
Homogeneity	0.961915	0.968218	0.959717	0.978025	0.95423	0.972941	0.947226	0.9734
Mean	0.003444	0.00351	0.003679	0.001982	0.003208	0.00244	0.001133	0.001078
Standard_Deviation	0.078017	0.078014	0.079985	0.066788	0.078027	0.078055	0.080062	0.066809
Entropy	1.797035	1.251166	1.959506	0.969317	2.300984	1.149188	2.688708	1.977195
RMS	0.078087	0.078087	0.080064	0.066815	0.078087	0.078087	0.080064	0.066815
Variance	0.006078	0.006079	0.006391	0.00446	0.006091	0.006106	0.006413	0.004464
Smoothness	0.957619	0.958383	0.961905	0.967939	0.954638	0.94119	0.886076	0.942601
Kurtosis	36.38611	43.74469	23.75865	77.07765	26.25241	49.94378	11.93987	53.1183
Skewness	2.94021	3.50774	2.054355	5.053549	1.985059	3.637179	0.830211	3.325072
IDM	0.750981	0.227072	0.470218	1.883483	1.534089	1.589721	0.329004	2.601781

From a single MR image, the following statistical features are extracted: Each of the following is a measure of variability: the Mean, the Standard Deviation, the Median Intensity, the Skew, the Smoothness, the Kurtosis, the Contrast, and the Correlation. This data is summarized in Table 2. During feature extraction, each image yields thirteen features. There are two steps to categorization: training and testing. There are 15 features from 12 benign and 12 malignant images that are provided to the classifier when it is being trained. A total of 85 images are supplied to the classifier for testing, with the SVM technique being used to categories them. A dangerous tumor was misclassified as a benign tumor using the suggested SVM classifier in Table 3, which correctly recognized 45 tumors. The suggested SVM classifier was able to correctly classify 98% of the time.

Table 3
Comparative analyses of SVM-KFCM values with other approaches

Parameter	Reff.[25] SVM-FCM	Reff.[20] SVM-FCM	Reff.[14] SVM	Proposed SVM-KFCM
Accuracy	95.4	97.8	95.45	98.1
MSE	-	-	0.0975	36.03
PSNR	-	-	58.24	10.35
Segmented area(pixels)	-	-	3849	11875

Table 3 shows that SVM estimates using KFCM are more practicable estimates than SVM–FCM or other approaches. This occurs as a result of the SVM with KFCM method's constant increase in accuracy.

Conclusion

Brain MR images are segmented using the KFCM and FCM algorithms, and the images are then classified into benign and malignant tumour groups using SVM. Table 1 shows algorithm performance parameters such as mean square error (MSE), processing time (s), PSNR value (dB), and segmented area for the 14 MR brain images utilized in this investigation. The statistical characteristics are recovered via wavelet decomposition when using the PCA approach. The training feature database comprises features that have been extracted from training images and electronically stored. 22 MR images of the brain are used to identify brain tumors using a newly developed supervised learning SVM classification method. The SVM classifier was 97.96% accurate with a 2.14 % error rate on experimental data.

Acknowledgment

The authors would like to thank the faculty members and staff in the Electronic Simulation laboratory at S.V.University College of Engineering, Tirupati for their encouragement ,co-operation and kindness..

Conflicts of interest

The author(s) declare(s) that there is no conflict of interest regarding the publication of this paper.

References

1. Abiodun, A. F. O. L. A. B. I. (2020). The Importance of Medical Imaging (X-RAY, EEG, PET etc) In the Understanding of the Effect of Manual Therapy on the Brain.
2. Achirul Nanda, M., Boro Seminar, K., Nandika, D., & Maddu, A. (2018). A comparison study of kernel functions in the support vector machine and its application for termite detection. *Information*, *9*(1), 5.
3. Ali, L., Niamat, A., Khan, J. A., Golilarz, N. A., Xingzhong, X., Noor, A., ... & Bukhari, S. A. C. (2019). An optimized stacked support vector machines

based expert system for the effective prediction of heart failure. *IEEE Access*, *7*, 54007-54014.

4. Ansari, M. A., Mehrotra, R., & Agrawal, R. (2020). Detection and classification of brain tumor in MRI images using wavelet transform and support vector machine. *Journal of Interdisciplinary Mathematics*, *23*(5), 955-966.
5. Bahadure, N. B., Ray, A. K., & Thethi, H. P. (2018). Comparative approach of MRI-based brain tumor segmentation and classification using genetic algorithm. *Journal of digital imaging*, *31*(4), 477-489.
6. Chakroun, R. W., Zhang, P., Lin, R., Schiapparelli, P., Quinones-Hinojosa, A., & Cui, H. (2018). Nanotherapeutic systems for local treatment of brain tumors. *Wiley Interdisciplinary Reviews: Nanomedicine and Nanobiotechnology*, *10*(1), e1479.
7. Coudray, N., Ocampo, P. S., Sakellaropoulos, T., Narula, N., Snuderl, M., Fenyö, D., ... & Tsirigos, A. (2018). Classification and mutation prediction from non–small cell lung cancer histopathology images using deep learning. *Nature medicine*, *24*(10), 1559-1567.
8. Despotović, I., Goossens, B., & Philips, W. (2015). MRI segmentation of the human brain: challenges, methods, and applications. *Computational and mathematical methods in medicine*, *2015*.
9. Goez, M. M., Torres-Madroñero, M. C., Röthlisberger, S., & Delgado-Trejos, E. (2018). Preprocessing of 2-dimensional gel electrophoresis images applied to proteomic analysis: a review. *Genomics, proteomics & bioinformatics*, *16*(1), 63-72.
10. Hameurlaine, M., & Moussaoui, A. (2019). Survey of brain tumor segmentation techniques on magnetic resonance imaging. *Nano Biomedicine and Engineering*, *11*(2), 178-191.
11. Hamid, M. A., & Khan, N. A. (2020). Investigation and classification of MRI brain tumors using feature extraction technique. *Journal of Medical and Biological Engineering*, *40*(2), 307-317.
12. Işın, A., Direkoğlu, C., & Şah, M. (2016). Review of MRI-based brain tumor image segmentation using deep learning methods. *Procedia Computer Science*, *102*, 317-324.
13. Krishnakumar, S., & Manivannan, K. (2021). Effective segmentation and classification of brain tumor using rough K means algorithm and multi kernel SVM in MR images. *Journal of Ambient Intelligence and Humanized Computing*, *12*(6), 6751-6760.
14. Kumar, S., Dabas, C., & Godara, S. (2017). Classification of brain MRI tumor images: a hybrid approach. *Procedia computer science*, *122*, 510-517.
15. Liu, Y., & Xie, M. (2020). Rebooting data-driven soft-sensors in process industries: A review of kernel methods. *Journal of Process Control*, *89*, 58-73.
16. Mohan, G., & Subashini, M. M. (2018). MRI based medical image analysis: Survey on brain tumor grade classification. *Biomedical Signal Processing and Control*, *39*, 139-161.
17. Permana, A. T., Suroto, N. S., Parenrengi, M. A., Bajamal, A. H., Lestari, P., & Fauzi, A. A. (2022). Current update on stroke ischemic management: Stem cell as emerging therapy. International Journal of Health & Medical Sciences, 5(1), 122-128. https://doi.org/10.21744/ijhms.v5n1.1851
18. Rajan, P. G., & Sundar, C. (2019). Brain tumor detection and segmentation by intensity adjustment. *Journal of medical systems*, *43*(8), 1-13.

19. Roy, B., Gupta, M., & Kumar, A. (2022). Target Detection from Brain MRI and Its Classification. In *Advances in Communication, Devices and Networking* (pp. 89-99). Springer, Singapore.
20. Shree, N. V., & Kumar, T. N. R. (2018). Identification and classification of brain tumor MRI images with feature extraction using DWT and probabilistic neural network. *Brain informatics*, *5*(1), 23-30.
21. Srinivas, B., & Rao, G. S. (2019). Performance evaluation of fuzzy C means segmentation and support vector machine classification for MRI brain tumor. In *Soft computing for problem solving* (pp. 355-367). Springer, Singapore.
22. Suryasa, I. W., Rodríguez-Gámez, M., & Koldoris, T. (2022). Post-pandemic health and its sustainability: Educational situation. *International Journal of Health Sciences*, *6*(1), i-v. https://doi.org/10.53730/ijhs.v6n1.5949
23. Ullah, Z., Lee, S. H., & Fayaz, M. (2019). Enhanced feature extraction technique for brain MRI classification based on Haar wavelet and statistical moments. *International Journal of Advanced and Applied Sciences*, *6*(7), 89-98.
24. van Moolenbroek, G. T., Patiño, T., Llop, J., & Sánchez, S. (2020). Engineering intelligent nanosystems for enhanced medical imaging. *Advanced Intelligent Systems*, *2*(10), 2000087.
25. Wang, S., Du, S., Atangana, A., Liu, A., & Lu, Z. (2018). Application of stationary wavelet entropy in pathological brain detection. *Multimedia Tools and Applications*, *77*(3), 3701-3714.
26. Willemink, M. J., Koszek, W. A., Hardell, C., Wu, J., Fleischmann, D., Harvey, H. & Lungren, M. P. (2020). Preparing medical imaging data for machine learning. *Radiology*, *295*(1), 4-15.
27. Yu, H., Sun, C., Yang, X., Zheng, S., & Zou, H. (2019). Fuzzy support vector machine with relative density information for classifying imbalanced data. *IEEE transactions on fuzzy systems*, *27*(12), 2353-2367.